JOURNAL OF PROPULSION AND POWER
Vol. 10, No. 6, Nov.–Dec. 1994

Development of Hypersonic Engine Seals: Flow Effects of Preload and Engine Pressures

Zhong Cai,* Rajakkannu Mutharasan,† and Frank K. Ko‡
Drexel University, Philadelphia, Pennsylvania 19104
and
Bruce M. Steinetz§
NASA Lewis Research Center, Cleveland, Ohio 44135

A new type of engine seal is being developed to meet the needs of advanced hypersonic engines. A seal made of emerging high-temperature ceramic fibers braided in a sheath-core construction is selected for study based on its low leakage rates. Flexible, low-leakage, high-temperature seals are required to seal the movable engine panels of advanced ramjet-scramjet engines. To predict the leakage through these flexible, porous seal structures as a function of preload and engine pressures, new analytical flow models are required. An empirical leakage resistance/preload model is proposed to characterize the observed decrease in leakage with increasing preload. Empirically determined compression modulus and preload factor are used to correlate experimental leakage data for a wide range of seal architectures. Good agreement is observed between measured and predicted values over a range of engine pressures and seal preload.

Nomenclature

A_c = cross-sectional area of the seal
A_y = yarn cross-sectional area
D_f = fiber diameter
E_{sl} = seal compression modulus
g_c = gravitational constant
L = seal length
$\dot{M}$ = mass leakage rate
M_w = molecular weight of gas
N_c = number of yarns in the core
N_s = number of yarns in the sheath
P_e = engine pressure differential, psig ($P_i - P_o$)
P_i = engine pressure upstream of seal, psia
P_o = engine pressure downstream of seal, psia
P_p = preload pressure, psig
R = leakage resistance, defined in Eq. (2)
R_g = universal gas constant
R_0 = leakage resistance at zero preload pressure
R_∞ = leakage resistance at infinite preload pressure
t = seal dimension
α = preload factor
ε = seal porosity
ε_0 = seal porosity at zero preload pressure
ε_{min} = seal minimum porosity at infinite preload pressure
θ = braiding angle
μ = gas viscosity

Subscripts
c = fiber core
s = braid sheath
sl = seal

Received May 16, 1993; presented as Paper 93-1998 at the AIAA/SAE/ASME/ASEE 29th Joint Propulsion Conference and Exhibit, Monterey, CA, June 28–30, 1993; revision received Jan. 26, 1994; accepted for publication Feb. 12. 1994.

*Research Associate, Materials Engineering Department.
†Professor of Chemical Engineering.
‡Professor of Materials Engineering.
§Senior Research Engineer, Structural Dynamics Branch. Member AIAA.

Introduction

RAMJET-SCRAMJET engines require sliding panel seals to prevent combustion gases from leaking past the articulating engine panels, similar to articulating panel seals of turbojet two-dimensional converging-diverging nozzles.[1] However, new seals are required for advanced hypersonic engines because of higher thermal loads and the need to seal larger engine sidewall distortions. As a point of comparison, turbojet nozzle seals developed under the augmented deflector exhaust nozzle program[2] used superalloy seals that sealed pressure differentials up to 30 psi, sealed sidewall distortions up to 0.030 in., and were cooled to 1200°F.

Hypersonic engine seals, however, are required to operate at higher temperatures (1500°F and above), seal high-pressure differentials (up to 100 psi), and seal larger sidewall distortions (up to 0.150 in.), as described in Ref. 3.

A seal concept that shows promise of meeting these challenging demands is the braided ceramic rope seal (developed at NASA Lewis Research Center). The braided ceramic rope seal structure consists of a high-density uniaxial core structure overbraided with an outer sheath for structural integrity, as shown in Fig. 1. Braided of emerging high-temperature ceramic fibers, this seal shows promise of operating hot and remaining flexible at temperatures up to 2000°F. Active preload means, such as the cooled metal bellows as shown, are used to preload the seal against the adjacent sidewall. As one would expect, increasing seal preload increases seal flow resistance, thereby limiting leakage flow through the seal. In high heat flux regions of the engines, the seals are cooled by transpiring coolant through the seals, as shown by the coolant flowing into the flowpath in Fig. 1. In this arrangement the seals act to limit purge gas to acceptable flow rates. For less severe locations, the seals can be used to limit parasitic leakage past the seals, in the reverse direction.

Accompanying the development of these engine seals, flow models are being developed to predict the seal leakage through these porous seal structures. These seal flow models can be used during the design process in one of two ways: 1) to predict

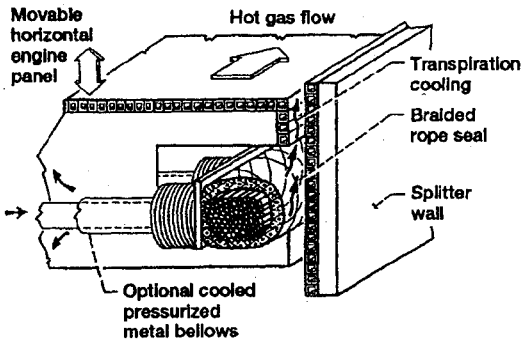

Fig. 1 Cross section of proposed engine seal.

performance losses associated with parasitic leakage through the seals, and 2) to predict purge coolant flow rates through these seals where ambient engine flow temperatures exceed the seal's operating temperature limit.

In an earlier paper[4] analyzing the seal leakage flow, mathematical models of leakage flow through the braided rope seals based on the Kozeny-Carman equation were proposed. The flow model enables prediction of gas leakage rate as a function of fiber diameter, seal porosity, gas properties, and pressure differential across the seal. Although the model predicts leakage rates satisfactorily, it does not account for changes in leakage rates at various lateral preload pressures.

The purpose of this article is to provide an analytical means of predicting the gas flow through these braided structures as a function of engine and preload pressures.

Theory

Seal Leakage Resistance

The braided rope seal structure shown in Fig. 1 presents an effective flow barrier between the high pressure P_i and low pressure P_o sides of the seal. Reference 4 provided the theoretical basis for modeling the one-dimensional flow through these seals based on the Kozeny-Carman equation with a fixed porosity ε. The mass flow for the seal structure was given as

$$\frac{\dot{M}}{L} = \frac{P_i^2 - P_o^2}{300(\mu R_g T/M_w g_c)(tL/A_c)[(1-\varepsilon)^2/\varepsilon^3(\phi D)^2]} \tag{1}$$

The braided seal flow resistance was defined as the rate of the differences in the squares of the pressures (driving potential) to the mass flow rate as

$$R = \frac{P_i^2 - P_o^2}{\dot{M}/L} \tag{2}$$

For simplicity in Ref. 4, R was assumed to be independent of the applied pressure difference and the preload applied to the seal.

Experimental evidence has shown that the effective seal flow resistance is dependent upon both the preload pressure and the engine pressure differential. Using Eqs. (1) and (2), the seal resistance is strongly dependent on the porosity as

$$R = \frac{K}{(\phi D_f)^2}\frac{(1-\varepsilon)^2}{\varepsilon^3} \tag{3}$$

where

$$K = 300\left(\frac{\mu R_g T}{M_w g_c}\right)\left(\frac{tL}{A_c}\right)$$

As will be shown herein, the seal porosity and the seal resistance are dependent upon the engine and preload pressures.

Resistance Preload Model

Establishing an analytical relationship between compression stress and strain based on the mechanical behavior of the thousands of fibers contained in these seal structures and the seal porosity would be immensely complex. Furthermore, the resulting expression may not provide an engineering model useful in predicting the seal leakage dependence on engine pressures and preloads. First, the fiber core and braided sheath should be considered separately. Second, in the seal core, all fibers are supposed to be perfectly aligned in the length direction, and the assumption of "point contact" may not be valid. Third, at the very low porosity level, a high transverse stress will be required to further compress the fiber assembly, and the compression resistance due to deformation of individual fibers may need to be considered. Therefore, a simpler empirical approach is proposed to describe the relationship between the seal leakage resistance, and the preload and engine pressures. Since both P_p and P_e change the seal resistance, both should be considered in evaluating seal performance. Expressing such an idea quantitatively gives

$$R = R_0 + (R_\infty - R_0)\left(1 - \exp\{-[\alpha P_p + (1-\alpha)P_e]/E_{sl}\}\right) \tag{4}$$

where R is the leakage resistance at a given preload pressure P_p and engine pressure P_e, R_0 is the leakage resistance at zero preload pressure $P_p = 0$ psig and "near-zero" engine pressure $P_e \approx 0$ psig, R_∞ is the maximum resistance at $P_p = \infty$ and $P_e = \infty$. The parameter E_{sl} is defined as the seal compression modulus, and α is a weighting factor of preload pressure contribution to the seal compression (abbreviated as preload factor). The expression captures the characteristics of the resistance-preload relationship observed in the experiments, namely the leakage resistance increases at a decreasing rate with increasing preload pressure. The leakage response behavior is governed by the seal compression modulus and the preload factor. The seal compression modulus and the preload factor, in turn, are governed by seal structure and the nature of the fiber material, and can be determined experimentally for a particular type of seal.

Letting ε_0 be the seal porosity with zero preload pressure and zero engine pressure, the leakage resistance at $P_p = 0$ psig and $P_e = 0$ psig can be estimated as

$$R_0 = \frac{K}{(\phi D_f)^2}\frac{(1-\varepsilon_0)^2}{\varepsilon_0^3} \tag{5}$$

When subjected to a hypothetical infinite preload, the seal is most tightly packed, and its porosity approaches the lowest possible value, denoted as ε_{min}. An analysis of the seal microstructure shows that the lowest seal porosity is 0.093, based on the architecture of hexagonal packing of cylindrical fibers. The maximum resistance can then be determined as

$$R_\infty = \frac{K}{(\phi D_f)^2}\frac{(1-\varepsilon_{min})^2}{\varepsilon_{min}^3} \tag{6}$$

With a rearrangement of the terms, Eq. (4) can be transformed to a linear equation for E_{sl} and α as

$$\frac{P_e}{\%(R_\infty - R_0/R_\infty - R)} = \alpha\frac{P_e - P_p}{\%(R_\infty - R_0/R_\infty - R)} + E_{sl} \tag{7}$$

Therefore, a linear regression method can be used to determine E_{sl} and α for the seal samples by using the experimental data (R, P_e, P_p). If the proposed model can describe the seal leakage response correctly, then experimental data will lie on a straight line in a transformed plot using Eq. (7). Graphical observations indicate there is some extent of data

scattering for different seals. Selection of a certain preload pressure range to perform linear regression calculation can give more accurate predictions within the interested pressure range.

In the calculation the initial seal resistance R_0 is obtained from Eq. (5) with the K from Eq. (3). The geometry transformation factor ϕ is chosen as 1.5.[4] D_f and the initial ε_0 are shown in Table 1. Similarly, the maximum resistance R_∞ is calculated from Eq. (6). The minimum seal porosity used in the calculation is $\varepsilon_{min} = 0.093$.

Experiments

Seal specimens used for this investigation were fabricated using a dense uniaxial core overbraided with several layers of two-dimensional braided sheath as indicated in Fig. 1. Seals were made of either E-glass fibers (seals A1, B1, D1, G1) or Nextel ceramic fibers (M6a, M6b, M6c). A summary of properties important to the current investigations are given in Table 1. More detailed architectural information for the E-glass and ceramic seals can be found in Refs. 4 and 5, respectively.

Flow Measurement

Seal specimens were mounted in a specially developed test fixture shown in Fig. 2, and were leak tested at room temperature under various inlet pressure conditions in the range of 5–80 psig. The pressure upstream of the seal was varied and the resulting leakage of gas (either air or helium) was measured. Lateral preloads were applied uniformly to the back of the seal with an inflatable rubber diaphragm at pressures from 0 to 240 psig. The flow resistance of the seal was computed from the ratio of the difference of squares of absolute pressures over the mass leakage rate using Eq. (2).

Porosity

Calculation of an initial resistance R_0 requires an initial porosity ε_0. The initial porosity used for the E-glass specimens fabricated for earlier studies were calculated using the following equation derived from fiber packing within braided structures as

$$\varepsilon_0 = 1 - [A_y(N_c + N_s/\cos\theta)/t^2] \quad (8)$$

where t^2 is the cross-sectional area of the installed seal.

Table 1 Seal specimen information

Specimen (material)	Seal porosity	Fiber diam, μm	Fiber modulus, $\times 10^6$ psi
A1 (E-glass)	0.48[a]	10	10.5
B1 (E-glass)	0.48[a]	10	10.5
D1 (E-glass)	0.42[a]	10	10.5
G1 (E-glass)	0.45[a]	10	10.5
M6a (Nextel 550)	0.562[b]	12	27.0
M6b (Nextel 440)	0.572[b]	12	27.0
M6c (Nextel 312)	0.515[b]	12	21.7

[a]Calculated porosity values.[4] [b]Compression-test measured porosity values.

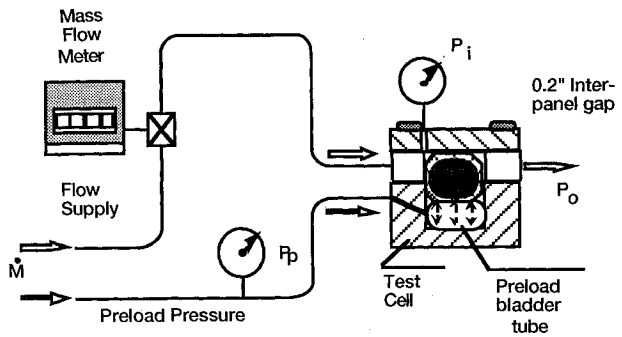

Fig. 2 Schematic of room temperature experimental apparatus.

Table 2a Resistance R_0 and R_∞ for seals A1, B1, D1, and G1

Seal	R_0, psia^2·s·ft/lb	R_∞, psia^2·s·ft/lb
A1	13,790	5,768,261
B1	13,790	5,768,261
D1	25,609	5,768,261
G1	18,722	5,768,261

Table 2b Compression modulus and preload factor for seals A1, B1, D1, and G1

Seal	α (air)	E_{sl}, psi (air)
A1	0.41	700
B1	0.70	1150
D1	0.58	760
G1	0.61	500

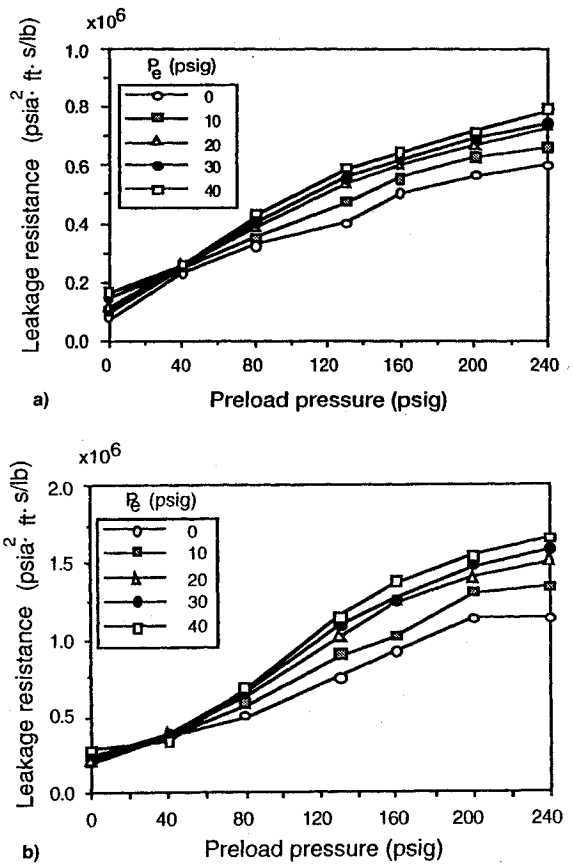

Fig. 3 Effect of preload and engine pressure on seal leakage resistance (air): a) seal A1 and b) seal G1.

Porosity for the Nextel® ceramic fiber seals were determined using a hybrid approach to better reflect the initial installed porosity of the seal. In this approach, samples of the seals were placed in a 0.5-in.-wide channel simulating the seal channel. This assembly was placed open side pointing-up, in a compression tester that applied increasing loads to the seal. Prior to loading, the initial seal height is measured. As the compression bar contacts the seal no significant load is measured. After the compression bar travels down some distance, the compressive load is measured. The position corresponding to this point of initial resistive load is also measured. The initial porosity is then calculated. Porosity determined using the above method are listed for each of the seals in Table 1.

Table 3a Resistance parameters R_0 and R_∞ for M6 series seals

Seal	R_0 (air), psia^2·s·ft/lb	R_∞ (air), psia^2·s·ft/lb	R_0 (helium), psia^2·s·ft/lb	R_∞ (helium), psia^2·s·ft/lb
M6a	4,233	4,005,714	33,375	31,582,673
M6b	3,834	4,005,714	30,226	31,582,673
M6c	6,745	4,005,714	53,180	31,582,673

Table 3b E_{sl} and α for M6 series seals

	Air		Helium	
Seal	α	E_{sl}, psi	α	E_{sl}, psi
M6a	0.20	2000	0.24	3810
M6b	0.20	1600	0.23	2940
M6c	0.26	1360	0.27	2520

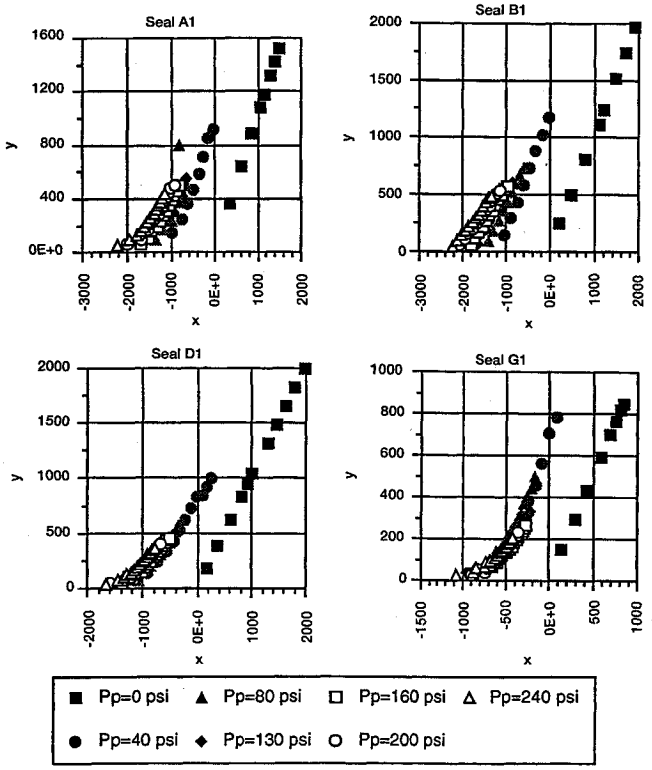

Fig. 4 Seal leakage data plotted on transformed coordinates to obtain α (slope) and E_{sl} (intercept).

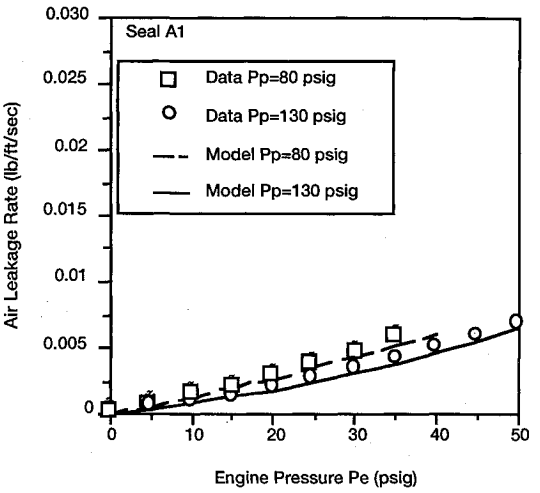

Fig. 5 Seal A1: measured air leakage rates vs pressure drops (symbols) compared to predictions (lines).

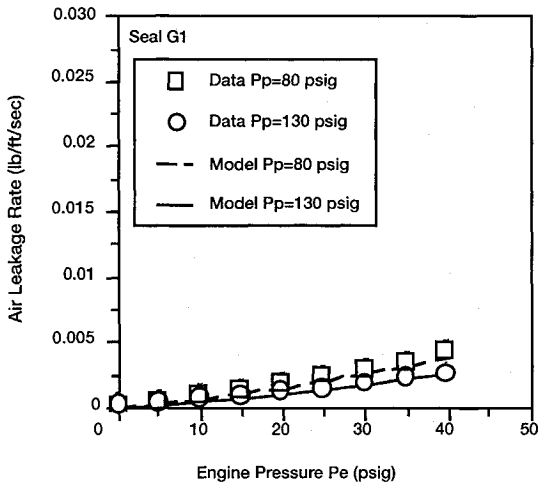

Fig. 6 Seal G1: measured air leakages rates vs pressure drops (symbols) compared to predictions (lines).

Results and Discussion

Leakage Resistance Pressure Dependence

Seal leakage resistance increases with increasing preload pressure and increasing engine pressure. Seal leakage resistances calculated with Eq. (2) are plotted for seals A1 and G1 in Fig. 3 demonstrating these trends. This behavior is typical of all of the seals examined.

Another observation made from Fig. 3 is that leakage resistance increases at a decreasing rate at high engine and preload pressure. In other words, the rate at which resistance increases slows as the seals reach lower porosity levels. This observation is the basis for the logarithmic form of the resistance preload model used in these current analyses.

R_0 and R_∞ Calculation

Initial R_0 and the maximum resistance R_∞ are required in using the proposed resistance preload model. In the proposed model the seal resistance at any preload and engine pressure R must be between the two limits of $R_0 < R < R_\infty$. R_∞ is calculated using the minimum porosity $\varepsilon_{min} = 0.093$ in Eq. (6), for the test gas being considered. The initial resistance R_0 is calculated using ε_0 found using techniques mentioned above and Eq. (5). The results of these calculations are given in Table 2a for the E-glass seals and Table 3a for the Nextel seals.

Correlation in Transformed Coordinates

The two parameters required for the resistance preload model to correlate the leakage data are α and E_{sl}. These parameters are evaluated by plotting the leakage data on transformed coordinates according to Eq. (7). Ideally the data should fall on a straight line with a slope corresponding to α and an intercept corresponding to E_{sl}.

The results of these calculations are plotted in Fig. 4 for seals A1, B1, D1, and G1. Except for the zero preload pressures, the data fall on a general trend line. This observation indicates that the final correlation is expected to be better at nonzero preloads where the seal is being slightly compacted. Using linear regression, the slope and intercept of this general trend line are the values used for subsequent analyses and are given in Table 2b for the E-glass seals. Similar exercises for the Nextel seals result in preload factors and compression moduli that are given in Table 3b.

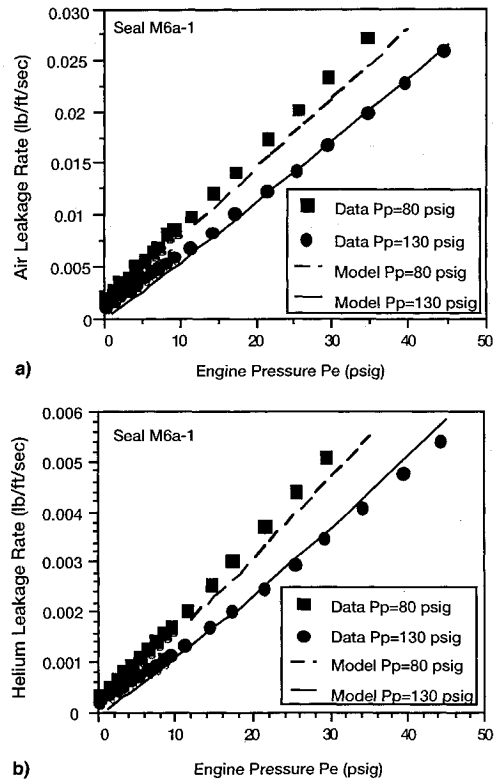

Fig. 7 Seal M6a-1: measured leakage rates vs pressure drops (symbols) compared to predictions (lines): a) air and b) helium.

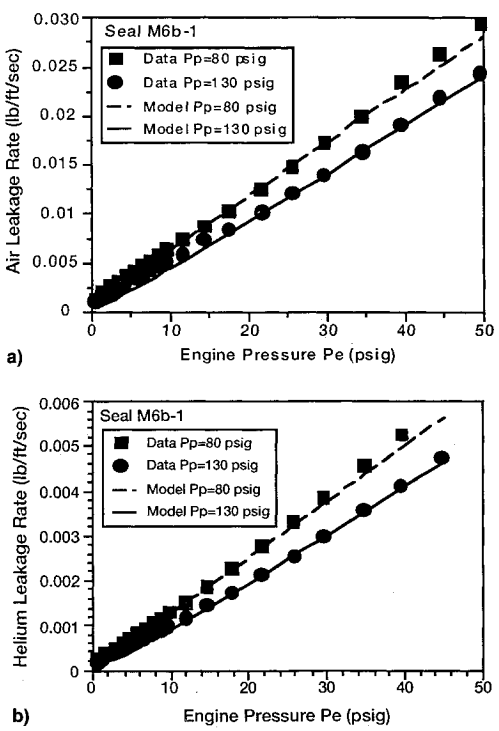

Fig. 8 Seal M6b-1: measured leakage rates vs pressure drops (symbols) compared to predictions (lines): a) air and b) helium.

Reviewing Table 3b, one notes that α is comparable for each of the test gases (air and helium), as expected. However, E_{sl} for air is lower than that of helium. It is unclear why this difference exists. It is possible that for the higher pressure differentials, the air leakage is flowing just outside of the laminar flow regime. As a result, it may be possible that part of the gas property dependence is being accounted for in the

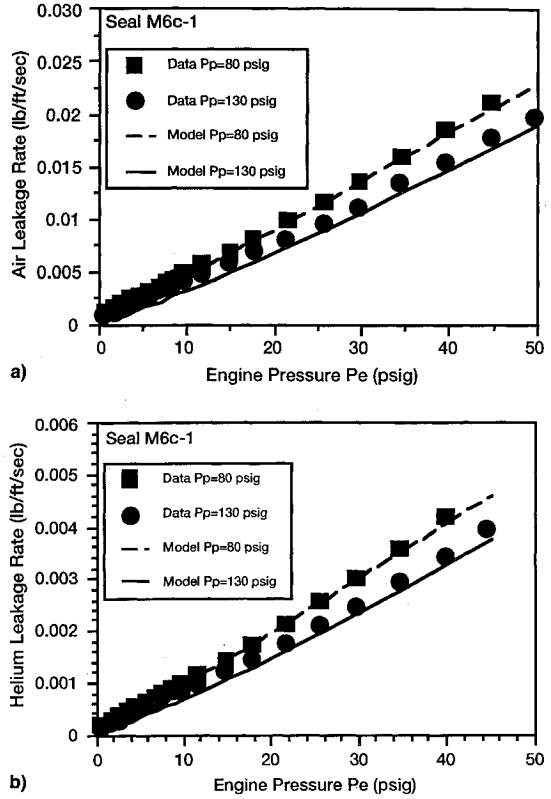

Fig. 9 Seal M6c-1: measured leakage rates vs pressure drops (symbols) compared to predictions (lines): a) air and b) helium.

E_{sl}. Although, as will be seen in the following, the correlation between the measured and predicted leakage rates for each gas is very good using the appropriate preload factor and compression modulus.

Final Correlation

After determining the required parameters, including R_0, R_∞, α, and E_{sl}, one is able to predict the seal leakage as a function of preload pressure, engine pressure, and gas type. The required parameters are substituted into Eq. (4) to determine the seal resistance R. With this R the mass flow rate can be evaluated for a given pressure differential using Eq. (2).

The results of these exercises for two E-glass seals A1 and G1 are shown in Figs. 5 and 6 for airflow, showing excellent agreement between measured and predicted leakage rates over the range of engine pressure differential examined. Similar agreement was observed for other E-glass seals.

A comparison between predicted and measured leakage results for the Nextel seals M6a, M6b, and M6c are given in Figs. 7–9. The agreement between predicted and measured results is again very good for both tested gases, air, and helium.

Summary

A semiempirical model has been presented for predicting leakage rates of braided rope engine seals as a function of preload pressure, engine pressure, and test gas. The model builds on previous work providing for an increasing seal flow resistance with increasing seal preload pressure and engine pressure. The logarithmic form of the resistance preload model characterize the observed variation of the seal leakage resistance with increasing preload and engine pressures using a two-term correlation. The preload factor provides a measure of the relative effects of preload and engine pressures on seal leakage. The seal compression modulus gauges the seal compressibility. The higher the compression modulus, the less the seal is deformed by transverse compression, and the less the leakage resistance is affected by the applied pressures. Correlation between the resistance preload model predictions and

measured data is excellent for a wide range of seal types (E-glass and ceramic), preload and engine pressures, and test gases (helium and air) examined.

Acknowledgments

This project is funded by NASA Lewis Research Center, Cleveland, Ohio. The authors wish to thank Xiaoming Tao, Susan Marr, Guang-Wu Du, Hon Wong, Dan Luu, and John McKelvie for their help in the seal design, fabrication, and testing.

References

[1]Kuchar, A. D., "Variable Convergent-Divergent Exhaust Nozzle Aerodynamics," *Aircraft Propulsion System Technology and Design*, edited by G. C. Oates, AIAA, Washington, DC, 1989, pp. 301–338.

[2]Anon., "Advanced V/STOL Propulsion Component Development. Vol. 1: Nozzle/Deflector. Final Report," Aircraft Engine Group, General Electric Co., R77AEG441-VOL. 1, Cincinnati, OH, Aug. 1977.

[3]Steinetz, B. M., "Evaluation of an Innovative High Temperature Ceramic Wafer Seal for Hypersonic Engine Applications," NASA TM-105556, Feb. 1992.

[4]Mutharasan, R., Steinetz, B. M., Tao, X. M., and Ko, F., "Development of Braided Rope Seals for Hypersonic Engine Applications, Part II: Flow Modeling," AIAA Paper 91-2495, June 1991.

[5]Steinetz, B. M., DellaCorte, C., Machinchick, M., Mutharasan, R., Du, G., Ko, F., Sirocky, P. J., and Miller, J. H., "High Temperature Dynamic Engine Seal Technology Development," NASA TM-105641, April 1992.